Available online at www.sciencedirect.com
ScienceDirect
International Journal of Pressure Vessels and Piping 85 (2008) 265–274
INTERNATIONAL JOURNAL OF Pressure Vessels and Piping
www.elsevier.com/locate/ijpvp

Influence of welding sequence on welding distortions in pipes

I. Sattari-Far*, Y. Javadi

Faculty of Mechanical Engineering, Amirkabir University of Technology, Tehran, Iran

Received 1 December 2006; received in revised form 25 July 2007; accepted 26 July 2007

Abstract

This paper presents a three-dimensional thermo-mechanical analysis to investigate the effect of welding sequence on welding deformations in pipe–pipe joints of AISI stainless-steel type. Single-pass TIG welding with V-joint geometry in pipes having a diameter of 274 mm and a thickness of 6.2 mm is studied here. Nine different welding sequences are analysed. The finite element results are compared with experimental data. It has been shown that selecting a suitable welding sequence can substantially decrease the amount of welding distortions in this pipe geometry.

Keywords: Finite element simulation; Welding distortion; Welding sequence; Welding modelling

1. Introduction

Pipe welding is widely used in a variety of engineering applications such as oil and gas industries, nuclear and thermal power plants and chemical plants. A non-uniform temperature field, applied during the welding process, produces deformation and residual stresses in welded structures. In pipe welding, ''diameter change'' is the most usual deformation type. After welding, the pipe diameter is changed from the original diameter because of welding shrinkage, as shown in Fig. 1. The diameter changes are not uniform in the circumferential direction of the pipe, and thus the pipe sections would not be circlular after the welding process. This non-uniformity of the pipe section is called ''ovality'', and is shown in Fig. 2.

The extent of deformations and residual stresses in welded components depends on several factors such as geometrical size, welding parameters, welding sequence and applied structural boundary conditions.

Finite element (FE) simulation has become a popular tool for the prediction of welding distortions and residual stresses. A substantial amount of simulation and experimental work focusing on circumferential welding with emphasis on pipe welding is available in the literature [1–12]. To reduce computational power requirements, assumptions such as rotational symmetry and lateral symmetry have been employed in numerical simulations [4–6]. These assumptions reduce the computational demand but may make the problem over-simplified by limiting the analysis to one section of the complete geometry and eliminate modelling of the welding sequence. Therefore, these simplified models are not capable of predicting the effects of weld start/stop locations, welding sequence and tack welds.

Fricke et al. [10] investigated multi-pass welding on a complete three-dimensional (3D) model for pipe weld, but nothing is mentioned about welding sequence. Tsai et al. [13] employed a 3D shell element and moving welding arc to simulate welding residual stresses in AISI 304 stainless-steel pipes. Li et al. [14] developed a full 3D FE model to simulate a multi-pass narrow gap girth welding process.

Recently, Jiang and co-workers [15] used a 3D FE model to predict temperature distributions in a multi-pass welded pipe branch junction. However, none of these works has simulated a fully 3D model for comparing deferent welding sequences in pipe welding.

This paper presents a parametric study to determine the effect of welding sequence on welding distortions. 3D FE simulation of a single pass butt-weld joint is performed using the FE code ANSYS [16]. Two stainless-steel pipes with an outer diameter of 273.7 mm, wall thickness of

*Corresponding author. Tel.: +98 21 64543426; fax: +98 21 6641 9736.
E-mail address: sattari@aut.ac.ir (I. Sattari-Far).

0308-0161/$ - see front matter © 2007 Published by Elsevier Ltd.
doi:10.1016/j.ijpvp.2007.07.003

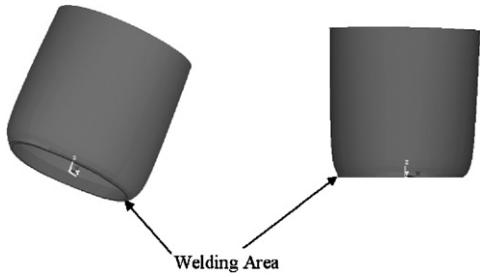

Fig. 1. Pipe diameter variation after welding.

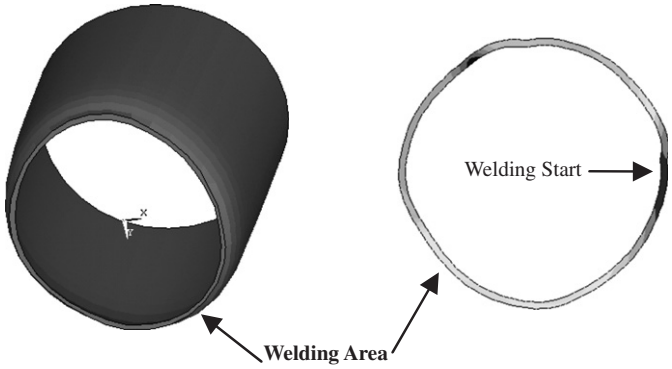

Fig. 2. Ovality after welding.

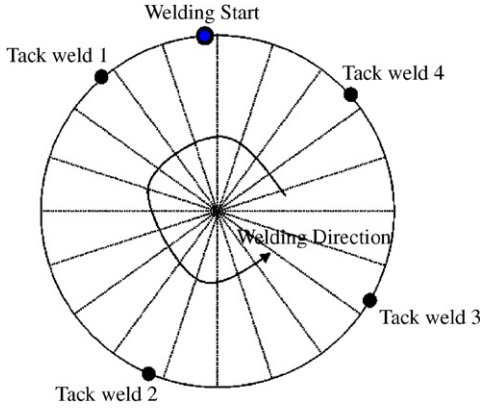

Fig. 3. Welding start and tack welds position.

6.2 mm and a length of 300 mm are welded together in a single-pass V-joint. Welding start locations and tack weld positions are shown in Fig. 3. A total of nine different sequences are analysed for the welding sequence of this pipe, as shown in Fig. 4. The case entitled as 1-seg, in which the weld is conducted entirely in one segment from the start to the final location, is chosen as the basic case here. This case has four tack welds, and is validated experimentally in this study. Any effects of tack welds on distortions and residual stresses are neglected in the analysis.

2. Modelling of physical phenomena

Numerical simulation of residual stresses and distortions due to welding needs to accurately take account of the interactions between heat transfer, metallurgical transformations and mechanical fields.

The phenomena involved in the heat input such as arc, material interactions as well as fluid dynamics in the weld pool are not accurately described. From the thermo-mechanical point of view, the heat input can be seen as a volumetric or surfaced energy distribution, and the fluid flow effect, which homogenizes the temperature in the molten area, can be simply taken into account by increasing the thermal conductivity over the fusion temperature.

The different phenomena involved and their couplings are given in Fig. 5. As no metallurgical transformation occurs in the 304 stainless steel considered in this paper, no detailed modelling of the melting is considered here.

2.1. Heat transfer analysis

The heat transfers in solids are described by the heat equation

$$\rho \frac{\mathrm{d}H}{\mathrm{d}t} - \mathrm{div}(\lambda \mathrm{grad}T) - Q = 0, \tag{1}$$

$$\lambda \mathrm{grad}T n = q(T,t) \quad \text{on } \partial\Omega_q, \tag{2}$$

$$T = T_\mathrm{p}(t) \quad \text{on} \quad \partial\Omega_t,$$

where ρ, H, λ and T are density, enthalpy, thermal conductivity and temperature, respectively. In Eq. (1), Q represents an internal heat source. In Eq. (2), n is the outward normal vector of domain $\delta\Omega$ and q the heat flux density that can depend on temperature and time to model convective heat exchanges on the surface. T_p represents a prescribed temperature. The heat input is represented by an internal heat source.

In the present study, the double ellipsoid heat source configuration proposed by Goldak et al. [17] is used, as shown in Fig. 6. As is seen, the front half of the heat source is the quadrant of one ellipsoidal source, and the rear half is the quadrant of another ellipsoid. In this model, the fractions of f_f and f_r of the heat deposited in the front and rear quadrants are needed, where $f_\mathrm{f}+f_\mathrm{r}=2$. The power density distribution inside the front quadrant is

$$q_\mathrm{f}(x,y,z) = \frac{6\sqrt{3}f_\mathrm{f}Q}{a_\mathrm{f}bc\pi^{3/2}} \mathrm{e}^{(-3x^2/a_\mathrm{f}^2)} \mathrm{e}^{(-3y^2/b^2)} \mathrm{e}^{(-3z^2/c^2)}. \tag{3}$$

Similarly, for the rear quadrant of the source the power density distribution inside the ellipsoid becomes

$$q_\mathrm{r}(x,y,z) = \frac{6\sqrt{3}f_\mathrm{r}Q}{a_\mathrm{r}bc\pi^{3/2}} \mathrm{e}^{(-3x^2/a_\mathrm{r}^2)} \mathrm{e}^{(-3y^2/b^2)} e^{(-3z^2/c^2)}. \tag{4}$$

Physically, these parameters are the radial dimensions of the molten zone in front, behind, to the side and underneath the arc. If the cross-section of the molten zone is known from the experiment, these data may be used to fix the heat source dimensions.

If cross-sectional dimensions are not available, the experience data given by Goldak et al. [17] suggest that it is reasonable to take the distance in front of the heat source